Materials Science & Engineering A 580 (2013) 133–141

Contents lists available at SciVerse ScienceDirect

Materials Science & Engineering A

journal homepage: www.elsevier.com/locate/msea

# Importance of diffusional creep in fine grained Mg–3Al–1Zn alloys

T.J. Lee [a], Y.B. Park [b], W.J. Kim [a,*]

[a] Department of Materials Science and Engineering, Hongik University, Mapo-gu, Sangsu-dong 72-1, Seoul 121-791, Republic of Korea
[b] Department of Materials Science and Engineering, Sunchon National University, 315 Maegok, Sunchon 540-742, Jeonnam, Republic of Korea

ARTICLE INFO

*Article history:*
Received 25 March 2013
Received in revised form
15 April 2013
Accepted 17 April 2013
Available online 29 April 2013

*Keywords:*
Mechanical characterization
Magnesium alloys
Grain refinement
Thermomechanical processing
Superplasticity

ABSTRACT

Deformation mechanisms of fine-grained Mg–3Al–Zn (AZ31) alloys that were prepared by using severe plastic deformation were identified at elevated temperatures between 473 K and 573 K by examining their stress–strain rate relations at different grain sizes and temperatures. Unlike the previous reports where grain boundary sliding has been suggested to be the rate-controlling deformation mechanism in the fine-grained AZ31 alloy, the current analysis indicated that Coble creep competes with grain boundary sliding and the contribution of Coble creep to overall strain rate increases as grain size decreases and temperature increases. Making the efforts to minimize grain growth during sample heating and tensile deformation is, however, important for observing Coble creep. Texture variation took place during the tensile deformation and differed depending on the type of dominant deformation mechanism operating under the given testing condition.



## 1. Introduction

There have been many efforts towards reducing grain size of Mg alloys to improve their strength at ambient temperatures and their superplasticity at elevated temperatures. The most popular "top–down" approach used for effective grain refinement in Mg alloys is severe plastic deformation (SPD), which includes equal channel angular pressing (ECAP) [1–3], accumulative roll bonding [4], multi-directional forging [5], friction stirring [6] and high-ratio differential speed rolling (HRDSR) [7,8]. According to the analysis of the relationship between strain rate and flow stress at different temperatures above 0.5 $T_m$ (where $T_m$ is the melting temperature) for a variety of Mg alloys with small grains a few micrometers in size, the typical value of strain rate sensitivity exponent ($m$) is ~0.5, and the activation energy for plastic flow is close to that value for grain boundary diffusion at low flow stresses [2,9]. Some Mg alloys with high volume fractions of second phase of particles or reinforcements exhibited $m$ values considerably smaller than 0.5, but after threshold-stress compensation, the $m$ value became ~0.5 [10]. These results suggest that grain boundary sliding (GBS) is the rate-controlling deformation mechanism for fine-grained Mg alloys at low stresses and is responsible for superplasticity.

For Mg alloys with small grain sizes, however, diffusional creep such as Nabarro–Herring (N–H) creep and Coble creep can be important because, like GBS, these mechanisms are also grain-size sensitive.

$$\dot{\varepsilon} = 14\frac{D_L}{d^2}\left(\frac{Eb^3}{kT}\right)\left(\frac{\sigma}{E}\right) \tag{1}$$

$$\dot{\varepsilon} = 14\frac{\pi\delta D_{gb}}{d^3}\left(\frac{Eb^3}{kT}\right)\left(\frac{\sigma}{E}\right) \tag{2}$$

Eq. (1) [11] describes the strain rate ($\dot{\varepsilon}$) by Nabarro–Herring creep, where $\sigma$ is the flow stress, $T$ is the absolute temperature, $D_L$ is the coefficient for lattice self-diffusion of Mg ($=1\times10^{-4}$ exp($-135{,}000/RT$) m$^2$ s$^{-1}$ [12], where $R$ is the gas constant ), $b$ is the Burger's vector ($3.21\times10^{-10}$ m [12]), $k$ is the Boltzmann constant, $E$ is the Young's modulus ($=4.3\times10^4$•[$1-5.3\times10^{-4}$•($T-300$)] MPa [12]) and $d$ is the grain size. Eq. (2) [11] depicts Coble creep, where $D_{gb}$ is the coefficient for grain boundary diffusion ($=7.79\times10^{-3}$ exp($-92{,}000/RT$) m$^2$ s$^{-1}$ [12]) and $\delta$ is the grain boundary width ($=2b$).

For SPD-processed Mg alloys with a typical grain size of 2 μm, the predicted strain rates for N–H creep and Coble creep at 5–10 MPa and 523 K ($D_L=3.29\times10^{-18}$ m$^2$ s$^{-1}$ and $D_{gb}=5.05\times10^{-12}$ m$^2$ s$^{-1}$) are $2.63\times10^{-7}$–$5.27\times10^{-7}$ s$^{-1}$ and $2.32\times10^{-4}$–$4.64\times10^{-4}$ s$^{-1}$, respectively. This result indicates that Coble creep predicts a significantly higher strain rate than N–H creep (by a factor of ~1000). More importantly, the calculated strain rates for Coble creep are in the strain rate range ($1\times10^{-5}$ s$^{-1}$–$1\times10$ s$^{-1}$) that can be covered by typical tensile test machines. For the same grain size and temperature, the calculated strain rates for Coble creep for aluminum and nickel (with $D_{gb}=3.57\times10^{-13}$ m$^2$ s$^{-1}$ and $2.30\times10^{-17}$ m$^2$ s$^{-1}$ [12], respectively) are $1.03\times10^{-5}$–$2.06\times10^{-5}$ s$^{-1}$ and $3.82\times10^{-10}$

* Corresponding author. Tel.: +82 2 320 1468; fax: +82 2 325 6116.
*E-mail address:* kimwj@wow.hongik.ac.kr (W.J. Kim).

0921-5093/$ - see front matter © 2013 Elsevier B.V. All rights reserved.
http://dx.doi.org/10.1016/j.msea.2013.04.061

–7.65 × 10$^{-10}$ s$^{-1}$, respectively, indicating that the probability of observing Coble creep in the typical strain rate range increases as $D_{gb}$ increases. Previously, however, Coble creep has rarely been observed in Mg alloys. Recently, Kim [13] showed that Coble creep can be important in ultrafine-grained AZ91 (Mg–9Al–1Zn) alloy.

Mg–3Al–1Zn (AZ31) is the most widely used wrought magnesium alloy because of its good combination of strength, ductility and corrosion resistance. Deformation mechanisms and superplasticity of fine-grained AZ31 alloys have been extensively studied, typically in the temperature range between 573 K and 673 K [2,6,9]. Some studies were conducted at temperatures below 573 K [14,15], but the details of the associated deformation mechanisms have been scarcely analyzed.

In this paper, we studied the deformation mechanisms of fine-grained AZ31 alloys at temperatures between 473 and 573 K and explored the possibility of and conditions for observing Coble creep as the rate-controlling deformation mechanism.

## 2. Experimental procedures

Commercial AZ31 (Mg–3Al–1Zn) alloy sheets with a thickness of 2 mm were used as the starting material. This material will hereafter be referred to as the as-received AZ31 alloy. HRDSR was performed on the as-received AZ31 alloy using a rolling mill with a roll diameter of 300 mm. The speed ratio of the upper to the lower roll was set at 2 (6 rpm:3 rpm). A cold AZ31 sheet was fed to hot rolls (423 K or 473 K) for a total reduction of 70% in the thickness through the two-step rolling process. The sheet was rolled to 0.8 mm and then rolled again to a final thickness of 0.6 mm. There was no rotation of the samples between the two passes. The two materials obtained after the second passes at 473 and 423 K will hereafter be referred to as HRDSR-1 and HRDSR-2 AZ31 alloys, respectively.

For the microstructure study, the normal direction (ND) and rolling direction (RD) planes of the samples were examined using optics after etching the samples in a solution of picric acid (4.2 g), water (10 ml), acetic acid (10 ml) and ethanol (70 ml). The grain sizes were measured by the linear intercept grain size method using image analysis software (Olympus analysis TS Material®). Electron back-scattering diffraction (EBSD) analyses were performed on the ND-RD planes of the samples with a step size of 50 nm. TSL version 5.31 was used as the analysis software, and data points with confidence index (CI) values lower than 0.1 were removed from the EBSD data. The grain sizes of the samples were measured based on the EBSD image maps for a tolerance angle of 15°.

For tensile testing at high temperatures, tensile specimens with a dog-bone geometry and 5 mm gauge length were used. Tensile elongation-to-failure tests were performed (under constant crosshead-speed condition) to evaluate the tensile ductility at several temperatures and strain rates. The strain rate change (SRC) tests were carried out in the crosshead speed range between 0.05 (or 0.015) and 30 mm/min at 473, 523 and 573 K. A pre-strain of ~0.15 was imposed at an initial strain rate of 4 × 10$^{-3}$ s$^{-1}$ before the SRC was applied to stabilize the microstructure. A strain of ~0.03 was applied between the strain rates followed by the pre-straining. The SRC test at each temperature was repeated consecutively, to confirm that the strain-rate–stress relation obtained from the SRC test was reliable. That is, if the stress–strain rate curves from the first and second (repeated) rounds overlap, then limited microstructural change can be assumed to have occurred during the SRC test. In the case of HRDSR-2 AZ31, additional SRC tests were conducted in the crosshead speed range between 0.05 and 0.3 mm/min to monitor the change in the local $m$ value and flow-stress as a function of strain. A strain of ~0.06 was applied between the strain rates. During the SRC and elongation-to-failure testing, the tensile jig was preheated to a testing temperature and the sample was then mounted onto the sample holder in the heated jig. It took 5 min for the jig to reach the testing temperature again. Then, the sample was allowed to equilibrate at the testing temperature for an additional 5 min before initiating straining. This tensile jig preheating was performed to minimize grain growth before the initiation of tensile loading. Microstructure and microtexture of the as-received, HRDSR-1 and HRDSR-2 AZ31 alloys were examined by EBSD just before the tensile loading to evaluate the change in grain size during the sample heating and holding period. Microstructure and microtexture of some tensile samples were also examined by EBSD in the gauge (at the center of the gauge or approximately 1 mm away from the fractured tip in the case of fractured samples) and grip regions after the tensile deformation.

## 3. Results and discussion

The optical images of the as-received, HRDSR-1 and HRDSR-2 AZ31 alloys are shown in Fig. 1(a)–(c). The linear intercept grain size ($d$) of the as-received material (6.1 μm) reduced significantly after deformation by HRDSR. The $d$ values of HRDSR-1 AZ31 and HRDSR-2 AZ31 alloys were measured to be 2.7 and 2.1 μm, respectively.

Fig. 2(a)–(c) shows the EBSD images of the as-received, HRDSR-1 and HRDSR-2 AZ31 alloys. Unlike the as-received AZ31 alloy, HRDSR-1 and HRDSR-2 AZ31 alloys reveal large portions of dark regions in their images, indicating the presence of high dislocation density and high internal stresses in their microstructure. The grain sizes of the three materials measured by EBSD were 6.3, 2.0 and 1.9 μm, which are reasonably similar to those measured by optics. All three materials have a strong basal texture with similar maximum basal texture intensities of 16.1–17.5.

Fig. 3 shows the true stress-true–strain curves for the as-received, HRDSR-1 and HRDSR-2 AZ31 alloys at different temperatures at a strain rate of 3.3 × 10$^{-4}$ s$^{-1}$. HRDSR-1 and HRDSR-2 AZ31 alloys exhibit lower flow stresses and higher strain hardening rates than the as-received AZ31 alloy. They also reveal larger tensile elongations when compared at the same temperature. These results indicate that high temperature tensile deformation behavior of AZ31 alloy depends on grain size.

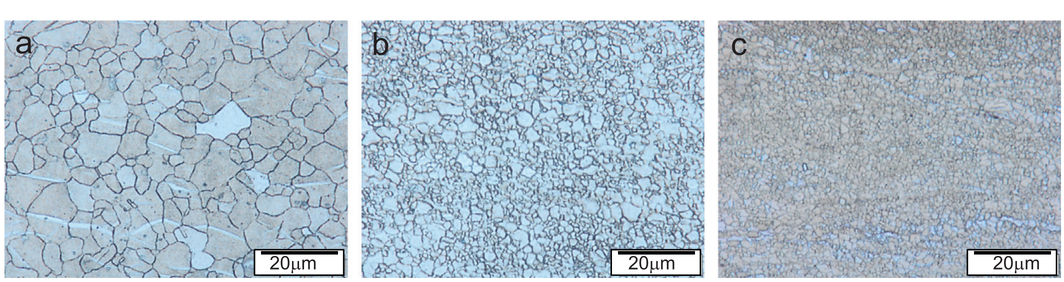


**Fig. 1.** The optical microstructures of the (a) as-received, (b) HRDSR-1 and (c) HRDSR-2 AZ31 alloys.